HAL
open science

Soot formation and oxidation during bio-oil gasification : experiments and modeling

Younes Chhiti, Marine Peyrot, Sylvain Salvador

To cite this version:

Younes Chhiti, Marine Peyrot, Sylvain Salvador. Soot formation and oxidation during bio-oil gasification : experiments and modeling. Journal of Energy Chemistry, 2013, 22, pp.701-709. 10.1016/S2095-4956(13)60093-5 . hal-00993565

HAL Id: hal-00993565

https://hal.science/hal-00993565

Submitted on 23 Mar 2018

HAL is a multi-disciplinary open access archive for the deposit and dissemination of scientific research documents, whether they are published or not. The documents may come from teaching and research institutions in France or abroad, or from public or private research centers.

L'archive ouverte pluridisciplinaire **HAL**, est destinée au dépôt et à la diffusion de documents scientifiques de niveau recherche, publiés ou non, émanant des établissements d'enseignement et de recherche français ou étrangers, des laboratoires publics ou privés.

Soot formation and oxidation during bio-oil gasification: experiments and modeling

Younes Chhiti[a*], Marine Peyrot[b], Sylvain Salvador[c]

a. LEGI, UJF-Grenoble 1/Grenoble-INP/CNRS, BP 53, Grenoble, F-38041, France;
b. CEA/DRT/LITEN/DTBH/LTB Laboratoire des Technologies pour la Biomasse 17, rue de Martyrs 38054, Grenoble, France;
c. Ecole des Mines d'Albi-Carmaux, Centre RAPSODEE, FRE CNRS 3213, Campus Jarlard, route de Teillet 81013, Albi, France

[Manuscript received February 8, 2013; revised April 2, 2013]

Abstract
A model is proposed to describe soot formation and oxidation during bio-oil gasification. It is based on the description of bio-oil heating, devolatilization, reforming of gases and conversion of both char and soot solids. Detailed chemistry (159 species and 773 reactions) is used in the gas phase. Soot production is described by a single reaction based on C_2H_2 species concentration and three heterogeneous soot oxidation reactions. To support the validation of the model, three sets of experiments were carried out in a lab-scale Entrained Flow Reactor (EFR) equipped with soot quantification device. The temperature was varied from 1000 to 1400 °C and three gaseous atmospheres were considered: default of steam, large excess of steam ($H_2O/C = 8$), and the presence of oxygen in the O/C range of 0.075–0.5. The model is shown to accurately describe the evolution of the concentration of the main gas species and to satisfactorily describe the soot concentration under the three atmospheres using a single set of identified kinetic parameters. Thanks to this model the contribution of different mechanisms involved in soot formation and oxidation in various situations can be assessed.

Key words
soot; gasification; pyrolysis; partial oxidation; bio-oil

1. Introduction

Due to continuous decrease in the amount and availability of conventional fossil fuels, it is becoming inevitable to search for new fuel sources. The renewable nature of biomass places it among the most attractive options. Using biomass as renewable feedstock would strongly contribute to decreasing greenhouse gas emissions due to neutral CO_2 balance. From a technical point of view, biomass feedstocks can be transformed into sustainable syngas (H_2+CO) or hydrogen by thermo chemical processes like gasification which includes several methods such as steam reforming (SR), partial oxidation (POX), and oxidative steam reforming (OSR) [1−3].

Soot formation is a major problem to face with in biomass thermal conversion. In a combustion process, soot formation results from incomplete combustion and typically occurs at fuel-rich stoichiometries. Soot formation is an active field of combustion research. This is not only because it remains a challenge from a fundamental point of view, but also because combustion-generated soot particles have serious environmental effects [4]. They are also associated with health risks since both polycyclic aromatic hydrocarbons (PAHs) that are precursors of soot and soot-associated organics have been identified to be carcinogenic. Moreover, soot may be a problem during operation of engines because it can lead to solid deposits [5].

Thus, the control of soot emission from combustion or gasification processes is a crucial issue that needs to be solved to avoid problems of deposits, to ensure syngas purity and to reduce harmful impacts to humans and the environment. Quantitative prediction of soot growth and subsequent oxidation mechanisms are critical to the development of approaches to control soot emissions [6,7]. Soot is produced in pyrolysis and combustion/gasification systems when conditions are such as to allow gas-phase condensation reactions of the fuel. The most accepted simple theory for soot formation is well described by Haynes and Wagner [8]. They assert that the pyrolysis of hydrocarbons produces smaller hydrocarbons, and in particular acetylene. The initial step is the formation of the first aromatic species from the aliphatic hydrocarbons, followed by the addition of other aromatic and alkyl species to give higher species, i.e. Polyaromatic Hydrocarbons (PAH). The continued growing of these PAHs results in the generation of small soot particles. In soot formation modeling, several principle proposals are known, which describe the nature of soot particle inception. According to them, different types of species are ranged as potential precursors, leading to soot

* Corresponding author. Tel: +33(6)60425664; E-mail: chhiti.younes@gmail.com

particle inception e.g., polyacetylenes or polyynes [9−12], and polycyclic aromatic hydrocarbons [13−16]. To model such a chemical process, it is desirable to use detailed chemical kinetic mechanisms including up to C_6 species, for example, the HACA-mechanism [17] and the extended HACA-mechanism [18]. An alternative approach for soot modeling is to use a semi-empirical model. The soot semi-empirical model here proposed is based on C_2H_2 as the precursor.

Until now, most experimental studies of sooting processes have been focused on fossil fuel combustion in diesel engines, and in diffusion flames. Thus, there are very few available data on soot formation from biomass and from bio-oil. The purpose of this paper is to propose a model able to describe as simply as possible the formation and the oxidation of soot during thermal conversion of bio-oil. The model is expected to describe the effect of temperature on soot formation and destruction over the range of 1000−1400 °C in three different kinds of atmosphere: inert, H_2O enriched and O_2 containing.

2. Experimental

2.1. Description of experimental device

Experiments were carried out in a laboratory scale Entrained Flow Reactor (EFR). It consisted in a vertical tubular reactor electrically heated by a total of 18 kW three-zone electrical furnace, and was able to reach 1600 °C in a 1m long isothermal reaction zone, as illustrated in Figure 1. The atmosphere gas was generated by feeding the controlled flows of nitrogen in a 2 kW electrical steam generator. This atmosphere gas was then preheated at 900 °C using a 2.5 kW electrical battery of heating elements before reaching the isothermal reaction zone. The EFR was equipped with a specially designed bio-oil spraying feeder. The feeder consisted of a 1 m long and 14 mm o.d. probe cooled with water at 30 °C. At its extremity a stainless steel nozzle was integrated, which allowed uniform distribution with fine atomization. The microscopic observation of droplets impacted on a surface indicates a size ranging between 10 and 100 μm. However, the majority of the droplets were much smaller and not observable.

The oil was fed with a syringe which is pushed automatically. The expected mass flowrate of 0.3 g·min^{-1} was too low for direct spraying. Therefore, a 3.5 NL·min^{-1} N_2 flowrate was used to entrain oil in the feeding probe and to ensure a thin spray of the oil. The spray of droplets was dispersed on the section of the 75 mm i.d. alumina reactor swept by 15 NL·min^{-1} of atmosphere gas. At 1760 mm downstream of the injection point, gas and solid residue were sampled by a

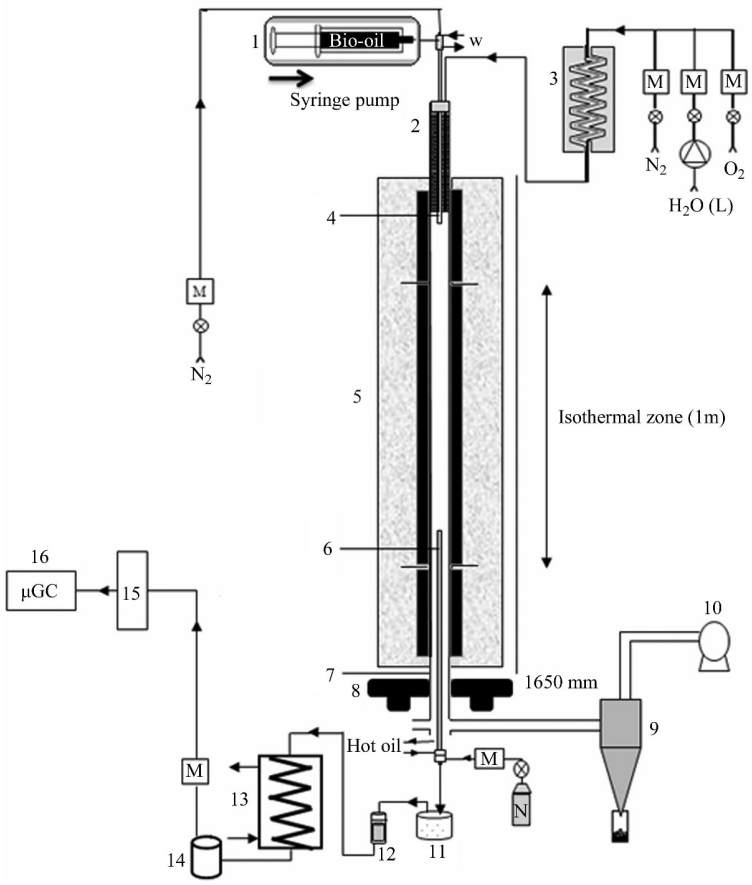

Figure 1. Scheme of the entrained flow reactor (EFR). 1—Injection system, 2—Electrical preheater, 3—Steam generator, 4—Water cooled feeding probe, 5—Three zones electrical furnace, 6—Oil cooled sampling probe, 7—75 mm i.d. alumina reactor, 8—Soot quatification device, 9—Cyclone collector, 10—Exhaust fan, 11—Hot settling box, 12—Hot particle collector (filter), 13—Water cooler, 14—Condensate collector, 15—Gas dryer, 16—Gas analyser; M—Mass flow meters and controllers, W—Water (feeder cooling)

hot-oil cooled probe. The injected atmosphere gas flowrate and the sampled gas flowrate were accurately measured using mass flow meters/controllers. Gas and solid residue were separated using a settling box and a filter, both heated to avoid water condensation. The water and potential remaining tar were first condensed in a heat exchanger, and non-condensable gases were forwarded to a micro-chromatograph analyser (GC) to quantify H_2, CO, CO_2, CH_4, C_2H_2, C_2H_4, C_2H_6, C_3H_8 and C_6H_6.

Laser extinction was used to make quantitative measurements of soot content in the produced gas. The optical thickness can be quantitatively related to the soot volumetric fraction through a linear relation. The coefficient associated to this relation was experimentally determined.

2.2. Feedstock

The feedstock used for all experiments was bio-oil produced by fast pyrolysis of mixture of hardwood (oak, maple and ash) in an industrial-scale fluidized-bed unit (Dynamotive, West Lorne, Ontario) and provided by CIRAD, France. Its physico-chemical properties have been measured (see Table 1). The water content of the bio-oil measured by Karl Fischer method (ASTM E203) is around 26 wt% which is in agreement with the average values reported in literature. It can be noticed that the solid particles content is rather high (2.3 wt%) while the ash content remains very low (around 0.06 wt%). This confirms that the solid particles mainly consist of high-carbon content char particles. These particles were entrained during bio-oil production by the gas stream to the bio-oil condensers. Ultimate analysis and LHV of the bio-oil are very similar to those of wood. From the ultimate analysis, the chemical formula of the bio-oil can be established as $CH_{1.18}O_{0.48}{\cdot}0.4H_2O$.

After the production, the bio-oil was stored at 5 °C in a fridge. Before experiments, it was filtered on a 30 m sieve to eliminate the largest solid particles which accounted for less than 0.01 wt% of the oil.

Table 1. Ultimate analysis and physico-chemical properties of bio-oil derived from hardwood fast pyrolysis

Ultimate analysis (wt%)				H_2O	Ash	Solids	LHV	Kinematic viscosity
C	H	O	N	(wt%)	(wt%)	(wt%)	(MJ/kg)	at 20 °C ($mm^2{\cdot}s^{-1}$)
42.9	7.1	50.58	<0.10	26.0	0.057	2.34	14.5	103

2.3. Model description and parameter setting

The GASPAR software computes the gasification of a solid spherical particle in a gaseous environment in Entrained Flow Reactor conditions. GASPAR has been developed successively by Van de Steene, Commandré, Cancès and Peyrot [19−22]. A one-dimensional (1D) laminar plug flow reactor is assumed in the model based on a Lagrangian approach. The whole flow is simulated considering a single particle, with possible distribution of particles of various diameters, and the associated gas volume. This particle and the gas volume sample constitute elementary part of the EFR's flow. The model simulates the time evolution of this sample along the reactor. The model is able to predict the evolution of several variables versus gas residence, namely, gas phase temperature, particle temperature, particle mass, gas species concentrations, soot yield and tar yield. All the differential equations are simultaneously time integrated through the Gear algorithm that can solve "stiff" ODE systems [23]. The whole model is included in a FORTRAN program.

For the present contribution, bio-oil droplets gasification is simulated as if droplets were solid particles. The droplets diameter is of about 10 μm. For such size, internal heat transfer can be neglected and the particle was considered as isothermal. The slip velocity between particle and gas can also be neglected here.

The GASPAR model is used here with the aim to describe soot formation and oxidation during gasification. It is based on the description of gas phase and bio-oil heating (radiative, conductive and convective heat transfer), bio-oil devolatilization, gas reforming and conversion of both char and soot solids. The gas phase reactions are computed using subroutines from the CHEMKIN II software [24]. For the present contribution, the chemical scheme used is the Skjøth-Rasmussen scheme (159 species, and 773 reactions) [25]. This model can also predict tar compounds evolution. Naphthalene has been taken as the reference compound to calculate tars in devolatilization products; this compound enters the detailed gas phase reactions. In the model, char can be oxidized via three heterogeneous reactions with O_2, H_2O and CO_2. Char conversion is modelled with the into-particle diffusion model where the chemical kinetics and the transport phenomena are taken into account through the Thiele diffusion modulus [26].

A four-step soot formation and oxidation model performs the soot computations using the mechanism:

$$C_2H_2 \longrightarrow 2C(soot) + H_2 \quad \text{Soot formation} \tag{1}$$

$$C(soot) + 0.5O_2 \longrightarrow CO \quad \text{Soot oxidation} \tag{2}$$

$$C(soot) + H_2O \longrightarrow CO + H_2 \quad \text{Soot gasification by } H_2O \tag{3}$$

$$C(soot) + CO_2 \longrightarrow 2CO \quad \text{Soot gasification by } CO_2 \tag{4}$$

2.4. Experimental conditions

The operating temperature was varied over the range of 1000−1400 °C. Gas atmosphere was preheated at 900 °C for all experiments. Bio-oil was then continuously fed by a feeding probe and injected into the reactor tube through a nozzle

by a nitrogen stream. The feeding rate of feedstock was of 0.3 g/min as explained previously, and three gaseous atmospheres were considered.

Firstly, the simplest situation of pyrolysis, i.e. in an inert atmosphere, was studied. In this case, the reactions involved are devolatilization, cracking, and some reforming and gasification by H_2O that is present in the fed bio-oil.

Secondly, excess of H_2O called steam gasification was studied. Gasification tests were carried out by supplying a mixed stream of nitrogen with steam. The steam to carbon molar ratio was S/C = 8.3 which was equivalent to 10 vol% of steam in the atmosphere gas.

Lastly, the presence of O_2 was explored. The so-called partial oxidation tests were carried out by supplying a mixture stream of nitrogen with O_2. The amount of O_2 was varied from very small amount to investigate a potential impact through radicals (O/C = 0.075), to large amount that may oxidize a significant part of bio-oil (O/C = 0.5). This is equivalent to 0.1−0.75 vol% of oxygen in atmosphere gas.

3. Results and discussions

In the following section, the yield of each main product is investigated separately. The experimental values are considered at first.

3.1. Profiles of product gas

Figure 2(a) shows gas species molar fractions at the bottom of the reactor versus temperature for pyrolysis, steam gasification and partial oxidation processes; Figure 2(b) plots gas species molar fractions at the bottom of the reactor versus O/C molar ratio for partial oxidation process at the temperature of 1200 °C.

3.1.1. H_2 production

The production of H_2 increased with temperature in all cases. The yields of H_2 in the exit gas varied in the order of steam gasification>pyrolysis>partial oxidation.

In the case of pyrolysis process, H_2 is thought to be mainly generated from the dehydrogenation (through the cleavage of C–H or O–H bond) of chemical compounds of bio-oil, and from the secondary decomposition of their pyrolyzed products (tars and hydrocarbon gas). Water contained by bio-oil can cause reforming reactions and favor the increase of H_2 with temperature.

In the presence of steam excess, the production of H_2 can be enhanced through steam gasifications of carbon (Equation 5) and condensable volatiles (Equation 6). The water-gas shift reaction can also contribute to the production of H_2 (Equation 7):

Carbon gasification

$$C + H_2O \longrightarrow CO + H_2 \tag{5}$$

Volatiles steam reforming

$$C_nH_mO_k + (n-k)H_2O \longrightarrow nCO + (n+m/2-k)H_2 \tag{6}$$

Water gas shift

$$CO + H_2O \longrightarrow CO_2 + H_2 \tag{7}$$

Both reactions (5) and (6) are endothermic, while reaction (7) is exothermic. Thus, high temperature will promote reactions (5) and (6), and low temperature will favor reaction (7) to shift towards the right.

On the other hand, the decrease in H_2 yields observed in partial oxidation runs with increasing O/C molar ratio suggests that combustion reactions predominate over steam gasification and water-gas shift reaction.

3.1.2. CO and CO_2 production

In the case of pyrolysis, CO and CO_2 yields are nearly stable between 1000 and 1200 °C. At higher temperature there is a slight increase in CO in parallel with a decrease of CO_2 which may be explained by Boudouard reaction:

$$C + CO_2 \longrightarrow 2CO \tag{8}$$

It is known that the production of CO in the pyrolysis process is mainly attributed to the decomposition of oxygen-containing functional groups in bio-oil.

In the steam gasification case, the water-gas shift reaction may also explain the increase of CO_2 and the decrease of CO between 1000 and 1200 °C. Above 1200 °C, carbon monoxide slightly increases. This may be explained by steam and CO_2 gasification of the solid carbon following Reaction (5) and the Boudouard Reaction (8) which would explain the slight decrease of CO_2.

On the other hand, unlike the pyrolysis and steam gasification cases, CO and CO_2 formation were significantly enhanced during partial oxidation tests. As O/C increases, the H_2 yield decreases while CO and CO_2 increase. This was caused by the increased amounts of oxygen which reacted with chemical species containing carbon and hydrogen and gave rise to CO_2, CO and H_2O following the reactions:

$$C + 1/2O_2 \longrightarrow CO \tag{9}$$

$$C_xH_yO_z + (x/2 - z/2)O_2 \longrightarrow xCO + (y/2)H_2 \tag{10}$$

$$C_xH_yO_z + (x + y/4 - z/2)O_2 \longrightarrow xCO_2 + (y/2)H_2O \tag{11}$$

3.1.3. Light hydrocarbon gas production

In Figure 2 only the major hydrocarbons CH_4 and C_2H_2 are shown. In all cases CH_4 is the most abundant species among the light hydrocarbon gases. Its production is maximal at 1000 °C and then decreases with temperature. It remains in trace amounts at 1300 °C and is below detection limit at 1400 °C. Its yield is greatly reduced when O/C ratio increases,

which shows that there is some partial oxidation. The trends are similar for C_2H_2.

The results of all simulations for the five temperatures 1000, 1100, 1200, 1300 and 1400 °C are shown in the same Figures as experiments (Figure 2a and 2b). As can be observed, the results obtained from the model are in very good agreement with experimental results, except for the C_2H_2 specie. This difference will be discussed later.

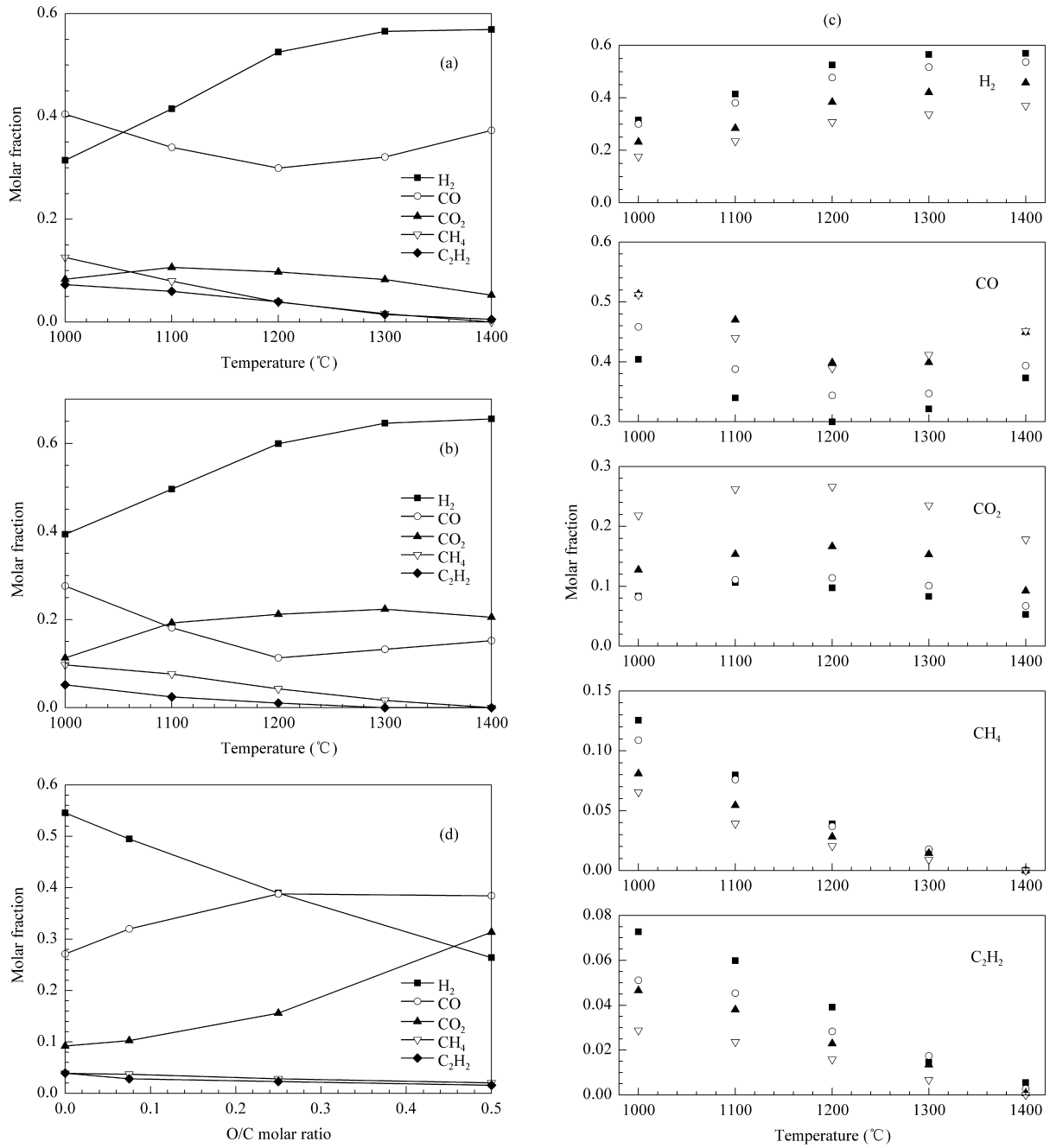

Figure 2. Gas molar fraction versus temperature: (a) pyrolysis case, (b) gasification case, (c) partial oxidation case (■ O/C=0, ○ O/C=0.075, ▲ O/C=0.25, ▽ O/C=0.5); and (d) gas molar fraction versus O/C molar ratio for partial oxidation process at 1200 °C

3.2. Soot production

The results of soot yields obtained in different experiments of pyrolysis, gasification, and partial oxidation are shown in Figures 3(a), 3(b) and 3(c), respectively.

In the case of pyrolysis (Figure 3a), an increase in temperature results in an increase in the soot yield. The increase in soot yield is accompanied by a decrease in the hydrocarbons gas yield as seen previously. This is in agreement with literature results [27−30].

The measured soot yield is close to zero at 1000 °C, while important amounts of C_2H_2 are present at the exit of the reactor. Above 1000 °C, a strong increase of soot yield with temperature is observed up to 1200 °C where the soot yield is 3.58×10^{-2} g/g. The soot yield measured at 1300 °C and 1400 °C is only slightly higher. This increase is accompanied by C_2H_2 decrease at the exit. The acetylene which is considered as the main soot precursor would react further to produce soot and hydrogen [31].

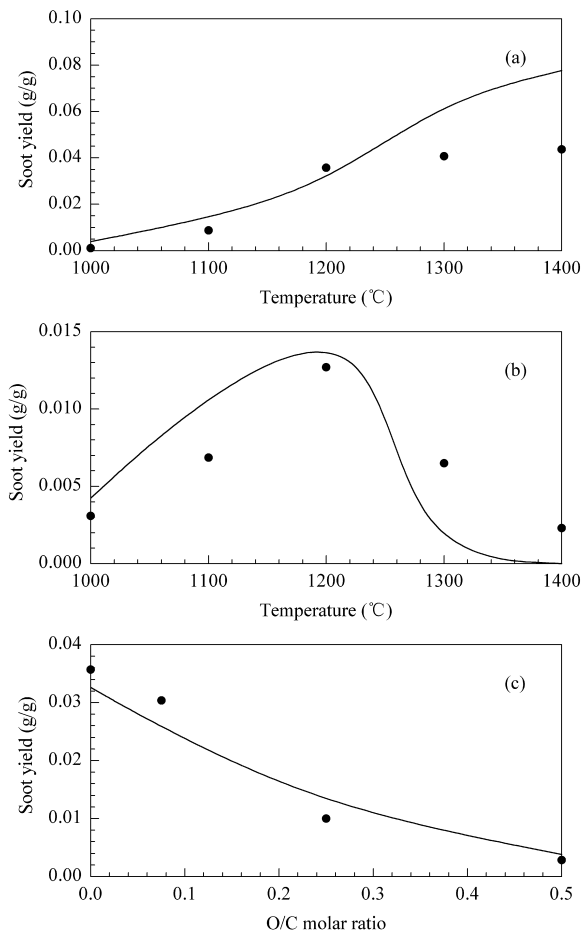

Figure 3. Soot yields versus temperature: (a) pyrolysis case, (b) gasification case. (c) Soot yields versus O/C molar ratio at 1200 °C: Partial oxidation case. Experiments (symbols) and modeling (lines)

The model satisfactorily predicts the soot formation at temperatures between 1000 °C and 1200 °C which tends to confirm the role of C_2H_2 in soot formation. Above 1200 °C the model predicts higher yields of soot than experiments. This may result from an incorrect calculation of the C_2H_2 gas phase concentration by the reaction mechanism. As can be seen in the product gas figure, the measured and calculated concentrations of acetylene show the same tendencies but with a gap.

In the gasification case, the soot yield is more than 3 times smaller than that in the pyrolysis case, as can be seen in Figure 3(b). The measured and calculated curves are both bell-shaped curves, showing that the model correctly describes the trend. At 1000 °C, experiment shows a low soot yield, which gets higher when reaction temperature increases and until the soot yield reaches a maximum of 1.27×10^{-2} g/g at about 1200 °C. Above 1200 °C, the soot yield strongly decreases. This decrease may be explained by steam and CO_2 gasification of soot following Reaction (5) and following the Boudouard Reaction (8) which would explain the slight decrease of CO_2 obtained in Figure 2(a), as well as the increase of H_2 and CO.

The limited formation of soot at high temperature due to the presence of water has been reported to result from changes in the radical pool [25]. Steam enhances the formation of hydroxyl radicals, through $H + H_2O \leftrightarrow OH + H_2$, and OH radicals may oxidize soot and also oxidize with C_2H_2 and therefore causes a decrease in the soot production. Water would therefore compete with C_2H_2.

In the partial oxidation case, from a thermodynamic point of view, soot formation can occur when fuel-rich conditions are present, i.e. when the O/C molar ratio is lower than 1. In the present experimental investigations the O/C molar ratio was varied from 0.075 to 0.5 at 1200 °C, because at this temperature the production of soot is the highest. As can be seen in Figure 3(c), the measured amount of soot strongly decreases with the O/C ratio under the conditions explored. This tendency is satisfactorily described by the model. According to the literature, when O/C molar ratio increases, most hydrocarbons are destroyed by oxidation or thermal decomposition, and numerous intermediate species are formed. In this way, a competition between the molecular growth and oxidative reactions occurs. Oxidative reactions lead to the formation of various oxygen-containing intermediates and products like CO, CO_2, and H_2O. As a result, the soot yield decreases compared with the case of pyrolysis.

3.3. Discussion: contribution of the model

In this section the model is used to discuss the results by identifying the contribution of each reaction to soot oxidation in the three situations (pyrolysis, steam gasification, partial oxidation). The prediction of the evolution of the gas species along the reactor also gives important information for understanding the transformation mechanisms.

(a) Pyrolysis situation

Calculations of soot yield are shown in Figure 4 versus temperature when oxidation reaction are activated and deactivated. In pyrolysis situation we note that the activation of the reaction of oxidation by CO_2 caused a negligible decrease in the soot yield. This oxidation was of about 3% at 1400 °C. Activation of the reaction with water has no effect at 1200 °C. However it causes a soot yield decrease of 26% at 1400 °C.

Figure 5 shows the profile of soot yield and C_2H_2 volumetric fraction along the reactor at 1200 °C. Acetylene curve shows its maximum close to the top of the reactor. This zone corresponds to the maximum of soot production rate as shown by the slope of the curve. Then the decrease in C_2H_2 yield is logically accompanied by an increase of soot content along the reactor, in agreement with the precursor role of C_2H_2.

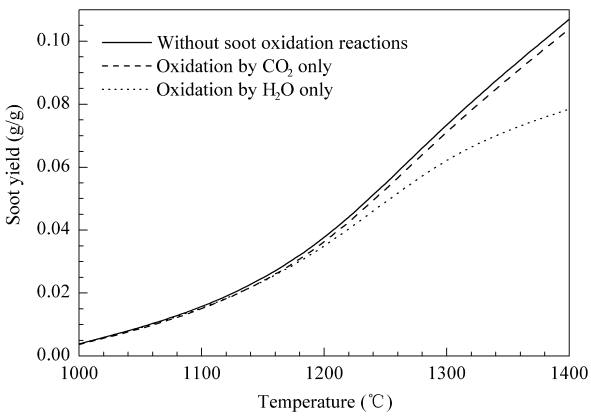

Figure 4. Soot yields versus temperature: modeling at different pyrolysis temperatures

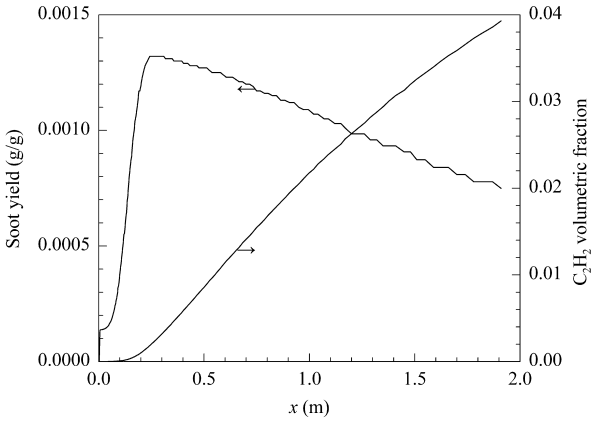

Figure 5. Profile of soot yield and C_2H_2 volumetric fraction versus the distance from nozzle during pyrolysis at 1200 °C

(b) Gasification situation

Calculations of soot yield are shown in Figure 6 versus temperature when oxidation reaction are activated and deactivated. We note that the activation of the reaction of oxidation with CO_2 caused a very small decrease in the soot yield. Activation of the reaction with water caused an almost complete oxidation of soot at 1300 °C and 1400 °C.

As previously reported, steam enhances the formation of hydroxyl radicals at high temperature. These radicals may oxidize soot and also consume C_2H_2 and therefore cause a decrease in soot production. The issue here is to distinguish the effect of steam on the oxidation of soot through the reforming of C_2H_2 and through the direct oxidation by H_2O.

The profiles of C_2H_2 volumetric fraction and the soot yield through the reactor at 1200 °C have been plotted in Figure 7 in three situations:

(i) without steam: this corresponds to the situation in which the production of soot is at its highest level.

(ii) with steam and deactivation of the steam gasification reaction: in this situation only the reforming of C_2H_2 occurs;

(iii) with steam and activation of the steam gasification reaction: in this situation both the decrease of soot production through the reforming of C_2H_2 and through the direct oxidation of soot by steam may occur.

Comparing (i) and (ii) shows that the presence of steam leads to a slight decrease of C_2H_2, and subsequently causes a slight decrease in soot production. However the activation of steam gasification in situation (iii) causes a significant soot oxidation. This proves that the oxidation of soot is mainly due to a direct gasification of soot by steam.

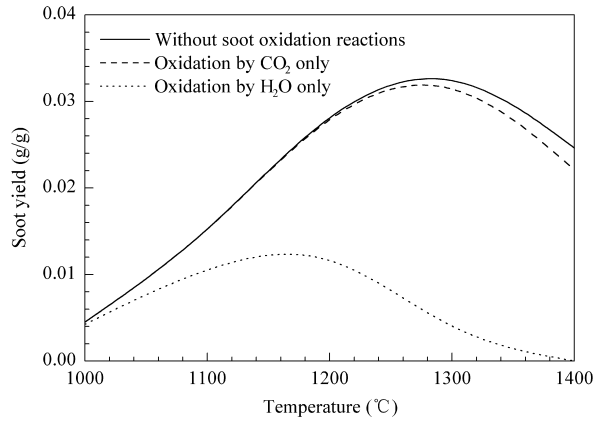

Figure 6. Soot yields versus temperature: modeling at different gasification temperatures

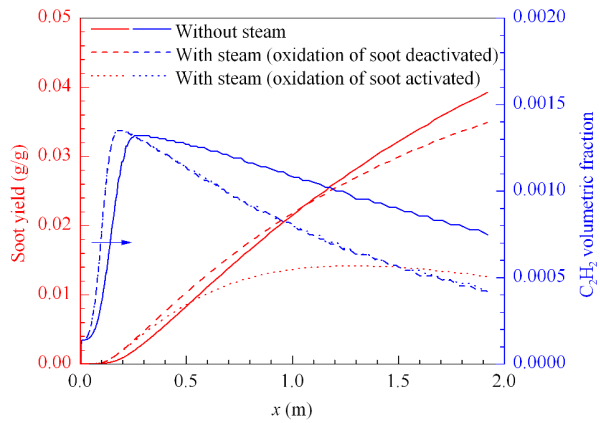

Figure 7. Profile of soot yield and C_2H_2 volumetric fraction versus the distance from nozzle during gasification at 1200 °C

(c) Partial oxidation situation

Calculations of soot yield are shown in Figure 8 versus temperature when oxidation reaction are activated and deactivated. None of the three oxidation reactions has a significant effect on soot yield.

As shown in Figure 9, O_2 seems to be consumed very quickly at the top of the reactor. Figure 10 shows the soot yield and C_2H_2 volumetric fraction along the reactor at 1200 °C at different O/C ratios. It can be noticed that when O/C increases C_2H_2 decreases in accordance with the O_2 consumption (Figure 10) and therefore less soot is produced. According to the model O_2 directly acts on C_2H_2 yield and thereafter on the amount of soot produced.

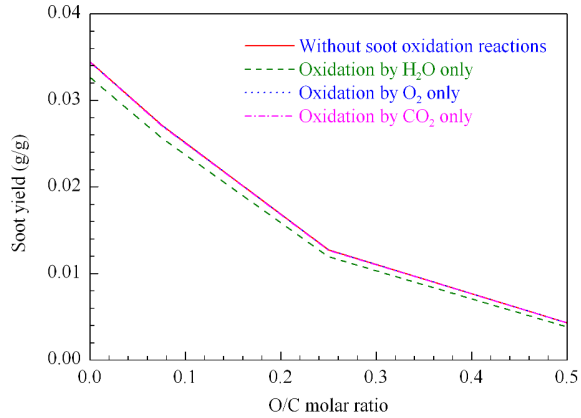

Figure 8. Soot yields versus O/C molar ratio at 1200 °C

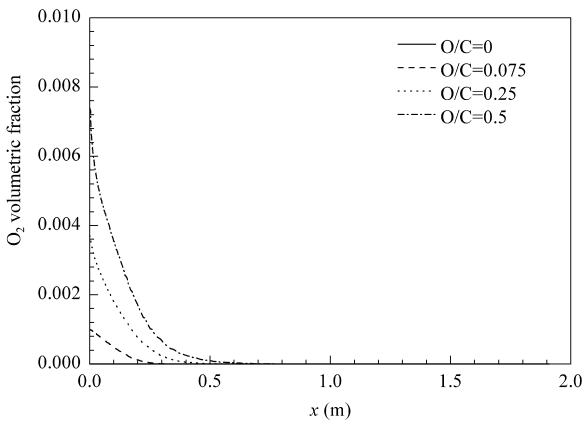

Figure 9. Profile of O_2 volumetric fraction versus a distance from nozzle at 1200 °C

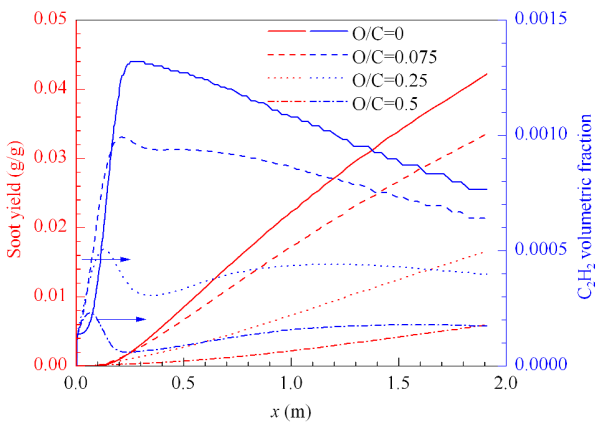

Figure 10. Profile of soot yield and C_2H_2 volumetric fraction versus the distance from nozzle during partial oxidation at 1200 °C—effect of O/C molar ratio

To sum up, based on the three considered situations, we found that among the three oxidation reactions only the steam gasification reaction exerts substantially effect on soot. Gasification with CO_2 has little effect and oxidation with O_2 has no effect.

4. Conclusions

The mechanisms of soot formation and oxidation are investigated through experiments under three different atmospheres: inert (pyrolysis), excess of steam (gasification) and in the presence of oxygen (partial oxidation). The proposed semi-empirical model is validated. It is based on detailed chemistry to describe the gas phase, on a single reaction based on C_2H_2 concentration to describe soot formation and on three heterogeneous reactions to describe soot oxidation. The approach appears to give satisfactory results. Indeed the amount of the main gases is very accurately predicted and the soot yield is correctly predicted. It has to be highlighted that a single set of identified parameters was used for all simulations.

The study confirms a strong influence of temperature on the mechanisms of soot formation and oxidation. Emphasis was also made on the effect of gasifying agents. Water in excess causes an almost complete gasification of soot at 1300 °C and 1400 °C. In the partial oxidation situation, at very low concentrations of O_2, the soot yield undergoes a slight decrease; an increase of O_2 amount greatly reduces the soot yield.

The contribution of each reaction of soot oxidation in the model is identified. CO_2 is shown to reduce only small quantities of soot. O_2 has no contribution to soot oxidation because it is consumed before soot is formed. Nevertheless, O_2 can be consumed by C_2H_2 and therefore causes a decrease in soot production. Only steam directly oxidizes the soot and causes their decrease.

Acknowledgements

The authors gratefully acknowledge the financial support from EnerBio Program of Fondation Tuck France, and express their gratitude to Mr. Bernard AUDUC technician in Ecole des Mines d'Albi-Carmaux for his assistance and contribution to experimental device design and operation.

References

[1] Cao L Y, Jia Z G, Ji S F, Hu, J Y. *J Nat Gas Chem*, 2011, 20(4): 377
[2] Liu H L, Hu J H, Wang H, Wang C, Li J Q. *J Nat Gas Chem*, 2012, 21(4): 374
[3] Zhao L M, Wang H, Qing S, Liu H L. *J Nat Gas Chem*, 2010, 19(4): 403
[4] Vedal S. *J Air Waste Manage Assoc*, 1997, 47(5): 551
[5] Bozzano G, Dente M, Faravelli T, Ranzi E. *Appl Therm Eng*, 2002, 22(8): 919
[6] Shan W J, Yang J L, Yang L H, Ma N. *J Nat Gas Chem*, 2011, 20(4): 384
[7] Shan W J, Ma N, Yang J L, Dong X W, Liu C, Wei L L. *J Nat Gas Chem*, 2010, 19(1): 86
[8] Haynes B S, Wagner H G. *Prog Energy Combust Sci*, 1981, 7(4): 229
[9] Homann H K, Wagner H G. *Proc Comb Inst*, 1967, 11: 371
[10] Frenklach M, Clary D W, Gardiner W C, Stein S E. *Proc Combust Inst*, 1985, 20(1): 887
[11] Kiefer J H, Vondrasek W A. *Int J Chem Kinet*, 1990, 22(7): 747

[12] Krestinin A V. *Khimicheskaya Fizika*, 1987, 6(3): 342
[13] Frenklach M, Wang H. *Springer*, 1994, 59: 165
[14] Griesheimer J, Homann K H. In: Burgess A R, Dryer F L ed. Proceedings of the 27th International Symposium on Combustion. 1998. 1753
[15] Appel J, Bockhorn H, Frenklach M. *Combust Flame*, 2000, 121(1-2): 122
[16] Richter H, Granata S, Green W H, Howard J B. *Proc Comb Inst*, 2005, 30(1): 1397
[17] Frenklach M, Wang H. 23rd International Symposium on Combustion, 1990. 1559
[18] Mauss F. [PhD Dissertation]. RWTH Aachen, 1998
[19] Van de Steene L. [PhD Dissertation]. INPT, 1999
[20] Commandré J M. [PhD Dissertation]. INPT, 2002
[21] Cancès J. [PhD Dissertation]. INPT, 2006
[22] Peyrot M, Dupont C, Chen L, Spindler B, Valin S, Cancès J. Biomass Conference Lyon, 2010
[23] Radhakrishnan K, Hindmarsh A C. Technical Report, LLnL report UCLR-ID113855. 1993
[24] Kee R J, Rupley F M, Miller J A. Technical Report, SAND87-8215B. 1990
[25] Skjøth-Rasmussen M S, Glarborg P, Ostberg M, Johannessen J T, Livbjerg H, Jensen A D. *Combust Flame*, 2004, 136(1-2): 91
[26] Villermaux J. 2édition Tec & Doc Lavoisier, 2-85206-759-5. 1993
[27] Alexiou A, Williams A. *Fuel*, 1995, 74(2): 153
[28] Alexiou A, Williams A. *Combust Flame*, 1996, 104(1-2): 51
[29] Mendiara T, Domene M P, Millera A, Bilbao R, Alzueta M U. *J Anal Appl Pyrol*, 2005, 74(1-2): 486
[30] Fletcher T H, Ma J L, Rigby J R, Brown A L, Webb B W. *Prog Energy Combust Sci*, 1997, 23(3): 283
[31] McEnally C S, Pfefferle L D, Atakan B, Kohse-Höinghaus K. *Prog Energy Combust Sci*, 2006, 32(3): 247